Synthesis of Monodispersed and Spherical SiO_2-coated Fe_2O_3 Nanoparticle

Yang-Su Han, Seon-Mi Yoon, and Dong-Kuk Kim*

Department of Chemistry, College of Natural Sciences, Kyungpook National University, Taegu 702-701, Korea
Received August 16, 2000

The preparation of nanocrystalline hematite, α-Fe_2O_3, particles and their surface coating with silica layers are described. The hematite particles with the size of 30~60 nm are firstly prepared by thermal decomposition of trinuclear acetato-hydroxo iron (III) nitrate complex, $[Fe_3(OCOCH_3)_7OH{\cdot}2H_2O]NO_3$, at 400 °C. Subsequently the hematite surfaces are coated with silica layers by a controlled hydrolysis and condensation reaction of TEOS with varying the TEOS concentration and pH. Monodispersed and spherical SiO_2-coated Fe_2O_3 particles with the average particle diameter of ~90 nm and extremely narrow size distribution can be obtained at the pH of 11 and the TEOS concentration of 0.68 M, which are found to be the optimum conditions in the present study in achieving the homogeneous deposition of silica layers on hematite surfaces. Diffuse reflectance UV-Vis spectra reveal that the characteristic optical reflectance of α-Fe_2O_3 particles is preserved almost constant even after coating the surfaces, suggesting that the SiO_2 layers can be regarded as protecting layers without degrading the optical properties of hematite particles.

Introduction

Iron oxides and hydroxides are indispensable materials because they are used widely as pigments, magnetic materials, magnets, anticorrosive agents, and catalysts.[1-5] Among the various kinds of iron oxides, hematite (α-Fe_2O_3), maghemite (γ-Fe_2O_3), and wûstite (FeO), α-Fe_2O_3 powders are of special interest as red inorganic pigments.[5] It is therefore considerable efforts are being made in preparing fine and monodispersed iron oxide powders exhibiting uniform particle size and morphology to meet technological need as well as to understand the fundamental phenomena of nano-sized oxide particles.[6]

The conventional approach to industrial inorganic pigments is solid state transformations by, for example, thermally decomposing iron salts or oxide-hydroxides. This is apparently unsuitable for producing nanosized α-Fe_2O_3 particles, which are required for numerous specific applications. Alternatively various chemical routes have thus been proposed to synthesize such an ultrafine α-Fe_2O_3 powder, including hydrothermal reaction method, sol-gel process, chemical coprecipitation, etc.[7-10] They involve synthesizing a reactive gel or precursor material, such as hydroxide and oxalate, followed by decomposing the gel or precursor into the designed crystalline phase at an intermediate temperature. In general, the chemically-derived oxide powders exhibit superior physico-chemical and particle characteristics to those of the powders prepared by conventional ceramic method. Since the optical properties of a given pigment depend in a sensitive manner on the size and shape of its particle, wet-chemical routes are suitable for producing homogeneous and fine color pigments with reproducible optical properties. In addition to the size and shape of inorganic pigment particles, dispersion behavior of the particles in aqueous and non-aqueous media is another critical parameter in evaluating the inorganic color pigments. Because a vast majority of color pigments are applied as the forms of fiber, wire, and thin-films, colloidal suspensions of colored pigments are highly required. For instance, α-Fe_2O_3 powder is a representative practical red-color pigment, which being used as color filter materials in constructing display devices to improve chromaticity and contrast.[11] In this application, color pigments should have sufficient dispersibility in proper solvents and high optical transmittance to obtain homogeneous and thin coating layers.

Recently, the preparation and characterization of monodispersed colloidal nanoparticles composed of a core particle coated by a shell of different, controlled composition have been received considerable attention, mainly because of the promising technological applications, but also due to their various physico-chemical properties.[12-17] The surface coating of core materials with a different one alters drastically the surface properties of the composite particles such as dispersibility, coagulation, adherence, etc. In the present study, the deposition of uniform silica layers on fine iron oxide particles by a controlled hydrolysis of tetraethoxysilicate (TEOS) is investigated in order to obtain a monodispersed red-color pigment of spherical nanoparticles with narrow size distribution.

Experimental Section

Materials. All chemical were reagent grade and were used without further purification. The staring materials used were ferric nitrate, $Fe(NO_3)_3 \cdot 9H_2O$ (Aldrich, 98+%), tetraethoxysilicate (TEOS, $Si(OC_2H_5)_4$, Aldrich, 98%), NH_4OH (25%-NH_3, Duksan), and anhydrous acetic acid (Aldrich, 99%).

Sample preparation. In the preparation of core hematite particles, a precursory trinuclear acetato-hydroxo iron (III) nitrate, $[Fe_3(OCOCH_3)_7OH \cdot 2H_2O]NO_3$, was prepared

*To whom all correspondence should be addressed. Tel. & Fax.: +82-53-950-5331, e-mail: kimdk@knu.ac.kr

according to the method reported previously.[18] Typically $Fe(NO_3)_3 \cdot 9H_2O$ (40.4 g) was added to 25 mL of absolute ethanol and then 70 mL of acetic anhydride was reacted by adding in small portions. When the reaction started with evolution of heat, the reactant was cooled in ice bath. After the all part of the acetic anhydride was reacted, the solution was cooled by ice and the resulting precipitate was separated by filtration, and dried at 80 °C for 24 h in vacuum oven. Finally, the iron acetato-hydroxo precursor was subsequently converted into α-Fe_2O_3 by thermal treatment under an ambient atmosphere.

The hematite particle obtained by calcining the iron precursor at 400 °C for 20 h was used as core α-Fe_2O_3 particles in the following coating process with silica using the hydrolysis of TEOS. In order to determine the conditions for the formation of uniform silica shells, the concentration of TEOS and reaction pH were varied in some limited range. In a typical coating process, a weighed amount of α-Fe_2O_3 powder (0.5 g) was dispersed in ethanol solution (50 mL) by ultrasonication for 30 min. to obtain iron oxide suspension. Silica source solution prepared separately by dissolving TEOS into ethanol solution (50 mL) was then mixed with the iron oxide suspension under vigorous stirring. In the mixing process, the mole concentration of TEOS was varied in the range of 0.04-3.0 M and the pHs of the mixed solutions were adjusted to 5 or 11 by adding NH_4OH. The mixed solution was then refluxed at 100 °C for 24 h with continuous stirring to induce homogeneous and dense SiO_2 layers onto hematite surfaces. Then the reaction products were separated by centrifugation, washed thoroughly with ethanolic aqueous solution to remove any extraneous species, and dried under vacuum for 24 h. Finally the dried samples were thermally treated at 400 °C for 5 h.

Characterization. All the powders obtained during various treatments were analyzed using a powder X-ray diffractometer (MacScience, MXP-3) equipped with Ni-filtered Cu-Kα radiation (λ=1.5418 Å). X-ray photoelectron spectroscopy (XPS) spectra were recorded with a Phi 5000 ESCA system (Perkin-Elmer) with an Al anode target at room temperature and a pressure of 1×10^{-7} Pa, and the energy was calibrated from the electron binding energy of the carbon 1s peak at 284.6 eV. Diffuse-reflectance UV-Vis spectra were obtained in the range of 400-800 nm with a UV-VIS-NIR spectrophotometer (CARY-5G). The particle size and morphology of the core iron oxides and the silicate coated ones were examined in a HITACHI-4200S field emission scanning electron microscope (FE-SEM) operated at 25 kV.

Results and Discussion

In the precursor route to crystalline α-Fe_2O_3 particle, the organic residue contained in the $[Fe_3(OCOCH_3)_7OH \cdot 2H_2O]NO_3$ precursor is thermally decomposed completely beyond 300 °C accompanied by a large exotherm. Figure 1 shows the evolution of crystalline phases depending upon the calcination temperature. As evidenced by the XRD, thermal treatment of the precursor at 300 °C for 20 h (a) leads to the conversion of precursory $[Fe_3(OCOCH_3)_7OH \cdot 2H_2O]NO_3$ into a well crystalline β-Fe_2O_3. Raising the temperature to 400 °C (b), the β-Fe_2O_3 phase transforms again into α-Fe_2O_3 one. Figure 2 represents the SEM image of the hematite powders which consisted of nanometer-sized particles with the size of 30-60 nm. The size distribution is quite homogeneous but the morphology is slightly irregular. A weak agglomeration of primary particles is also visible owing to the particle sintering during the firing process.

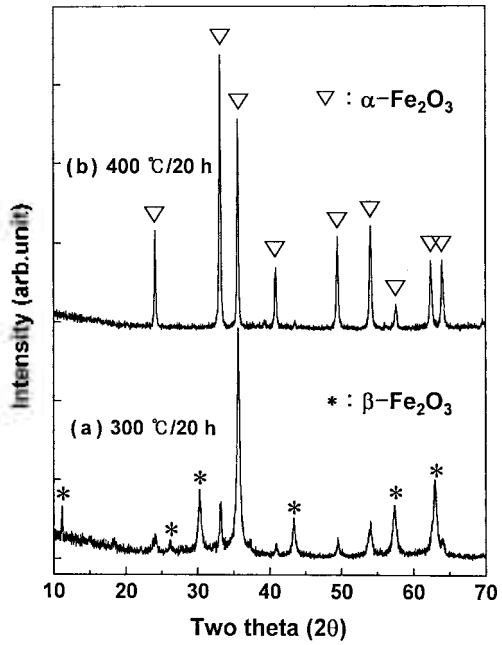

Figure 1. Powder X-ray diffraction patterns of iron oxide particles.

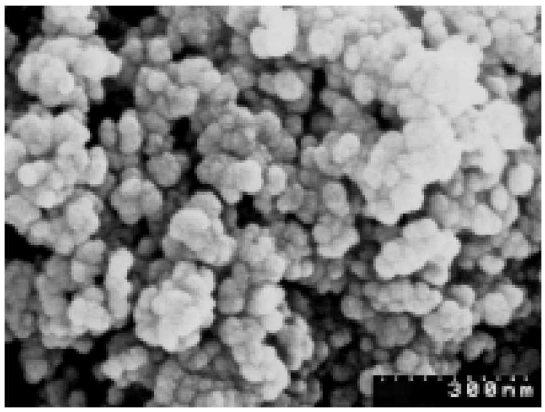

Figure 2. Scanning electron micrograph of the hematite particles obtained after calcination at 400 °C for 20 h.

Such prepared hematite nanoparticle were subjected to coating with silica through a controlled hydrolysis reaction of TEOS in the presence of water and catalyst (ammonia). The scanning electron micrographs in Figure 3 and Figure 4 reveal that the morphology, size and its distribution of core particles can be greatly altered by the surface deposition of silica layers. Figure 3 represents the SEM photographs for the SiO_2-coated Fe_2O_3 particles obtained at pH=5 and variable TEOS concentrations. In the lower TEOS concentration

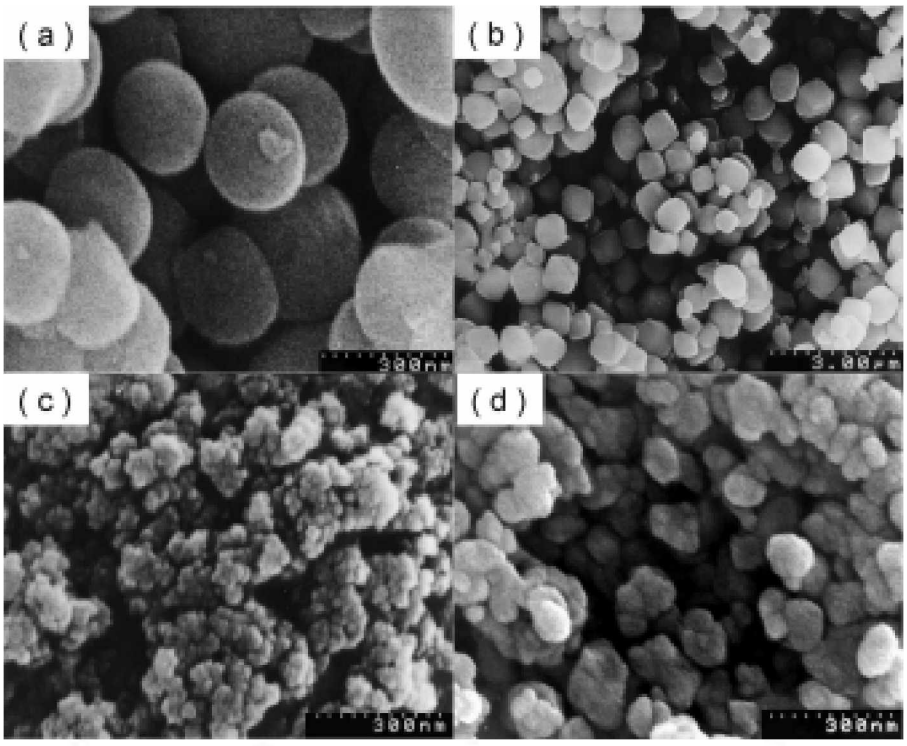

Figure 3. Scanning electron micrographs of the SiO_2-coated Fe_2O_3 particles prepared at pH=5 and various TEOS concentrations of (a) 1.37 M, (b) 2.10 M, (c) 3.00 M, and (d) 1.37 M without NH_4OH catalyst, respectively.

(1.37 M, Figure 3(a)), monodispersed spherical particles of ~150 nm are obtained. Remarkably the composite particles have extremely narrow size distribution. While the higher TEOS concentration (2.1 M, Figure 3(b)) in the coating process leads to the formation of monodispersed composite particles with cube-type morphology and sub-micron size (0.6-0.9 mm). When the TEOS concentration exceeds a certain level (>2.5 M of TEOS), spherical silica particles aggregated severely are produced separately (Figure 3(c)). In addition, a simple mixing of α-Fe_2O_3 with TEOS in the absence of catalyst (NH_4OH) seems not to be efficient to achieve homogeneous coating, instead irregular and severely agglomerated particles are observed (Figure 3(d)).

Figure 4 shows the SEM images for the coated particles prepared at pH=11. When the hydrolysis reaction of TEOS was carried out at the lower TEOS concentration of 0.04 M the coated particles have irregular morphology (Figure 4 (a)). The emergency of extremely small SiO_2 particles at the surface of Fe_2O_3 ones indicates that the inhomogeneous precipitation of SiO_2 is occurred under the lower TEOS concentration. Upon heating the mixed particles at 400 °C (Figure 4 (b)), the surfaces become smoothed due to the infiltration of SiO_2 layers into Fe_2O_3 matrix, but the irregular particle morphology still remains. Remarkably the size distribution and morphology are greatly improved when the hydrolysis reaction performed at the higher TEOS concentration (0.68 M). Monodispersed and spherical SiO_2-coated Fe_2O_3 particles are obtained as clearly can be seen from the Figure 4(c). The coated particles have average particle diameter of ~90 nm and extremely narrow size distribution. Therefore, it can be said that the higher TEOS concentration (0.68 M) is more favorable for achieving a homogeneous silica coating on hematite surfaces rather than the lower concentration. Lower concentration seems to be insufficient for obtaining enough coverage of hematite by silica, whereas if the TEOS concentration proceeds above the value (0.68 M), the individual silica precipitation would be unavoidable as observed in Figure 3(c). It is also worthy to note here that even after thermal treatment at 400 °C the size and morphology of the coated particles remain almost constant without significant particle agglomeration (Figure 4(d)). Since the silica layers possess high thermal resistance they act as protecting layers against the thermal sintering of the core hematite particles, which prevent form coalesening the nano-size core particles during the calcination.

In the coating at pH=5, the hydrolysis and subsequent condensation of hydrolyzed TEOS on surface metal hydroxyls occurs in the presence of water and catalysts as can be described: [12]

$$\alpha\text{-}Fe_2O_3 + Si(OC_2H_5)_4 + NH_3 + 2H_2O \rightarrow \alpha\text{-}Fe_2O_3 + SiO_2 + 4C_2H_5OH + NH_3$$

With controlled hydrolysis of TEOS, a Fe-O-Si chemical linkage is established between surface iron atoms and TEOS, followed by lateral polymerization, and finally formation of a three-dimensional network *via* siloxane bond formation (Si-O-Si) with increasing TEOS concentration and degree of hydrolysis. In the present study, 1.37 M of TEOS is found to be optimum for preparing monodispersed and spherical coated particles within our experimental con-

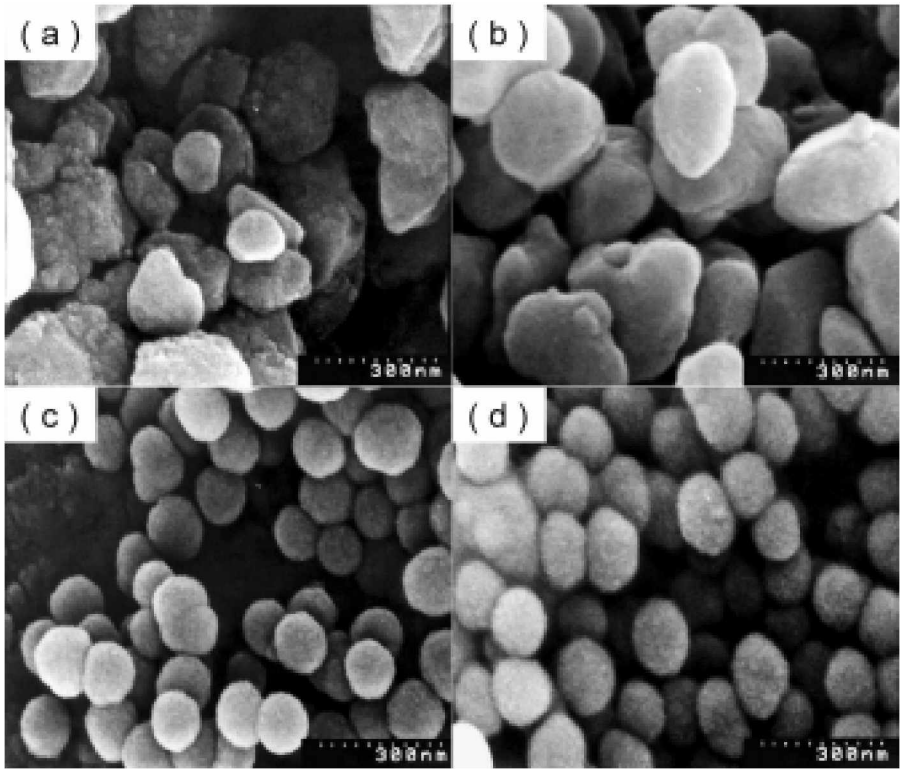

Figure 4. Scanning electron micrographs of the SiO_2-coated Fe_2O_3 particles prepared at pH=11 and the TEOS concentration of (a) 0.04 M and (c) 0.68 M, respectively. The micrographs of (b) and (d) represent the images for the samples of (a) and (c) calcined at 400 ℃ for 5 h, respectively.

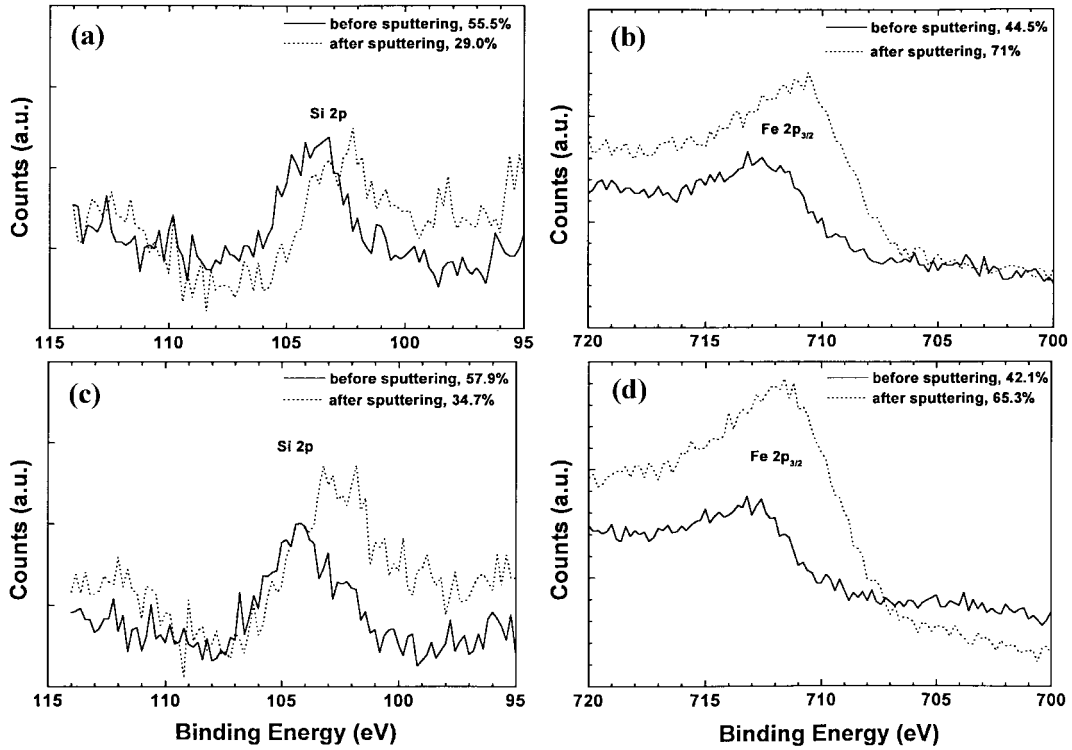

Figure 5. Si 1s ((a) and (c)) and Fe 2p ((b) and (d)) X-ray photoelectron spectra for the coated particles before (solid line) and after (dotted line) Ar ion bombardment.

ditions.

In contrast, when the coating is performed at quite basic condition (pH=11), higher TEOS concentration leads to a prompt precipitation of individual silica particles owing to

its higher level of supersaturation. In general, therefore, the lowest supersaturation level is required for homogeneous coatings.[16] In order to achieve the homogeneous deposition of silica layers, the homogeneous (silica) nucleation in the initial stage of deposition reaction should be suppressed, followed by heterogeneous coatings (hematite-silica), and finally homogeneous (silica) nucleation. Here, the homogeneous silica nucleation at the initial stage of reaction can be avoided by careful control of silica supersaturation level just above the critical concentration of heterogeneous coatings on hematite, which is determined to be the concentration of 0.68 M-TEOS in the present study.

In order to get insight into the surface composition of the coated particles, XPS spectra were recorded for the samples before and after argon ion bombardment as shown in Figure 5. At first the presence of silicon bands at around 103.4 eV on the spectra of coated particles before the ion bombardment (Figure 5(a) and (c)) supports the successful coatings on hematite surfaces. The Fe $2P_{3/2}$ binding energy observed at 713 eV for the samples before ion-sputtering (Figure 5(b) and (d)) corresponds to the Fe^{3+} species distributed in Fe_2O_3-SiO_2 matrix.[17,19,20] After ion-sputtering the binding energy shifts to 710.8 eV, which shows in good agreement with that of pure α-Fe_2O_3.[19,20] The relative fractions of Si and Fe at the surfaces before the ion-bombardment are 44.5% and 55.5%, respectively, for the sample prepared at 0.68 M-TEOS and pH=11 (Figure 5(a) and (b)), indicating that the composition at or near the surface of the particles is mainly composed of SiO_2-rich phase. While after ion-bombardment the fraction of Fe increases to 71%, suggesting that the core particles mainly consisted of hematite. For the sample obtained at pH =5 and TEOS concentration of 1.37 M, a similar change is observed before and after ion bombardment. Only the fraction of Fe species lower than that of the sample prepared at pH=11 and 0.68 M-TEOS both before and after ion-sputtering. Therefore it is likely that the thicker SiO_2 layers are formed on hematite surfaces at the lower pH of 5 and higher TEOS concentration of 1.37 M.

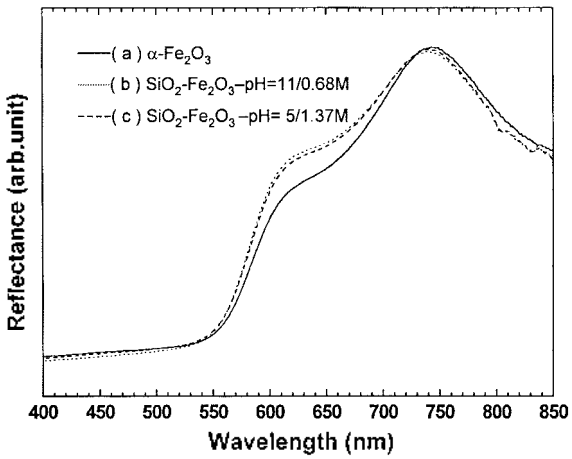

Figure 6. Diffuse reflectance UV-Vis spectra for the pure (a) α-Fe_2O_3 and SiO_2-coated Fe_2O_3 particles obtained at the conditions of (b) pH=5/1.37 M-TEOS and (c) pH=11/0.68 M-TEOS, respectively.

The solid reflectance UV-Vis spectra for the pure α-Fe_2O_3 and SiO_2-coated Fe_2O_3 particles are compared in Figure 6 to investigate the influence of the surface coating on optical properties. As clearly can be seen from the figure, the characteristic optical reflectance of α-Fe_2O_3 particles is preserved almost constant even after coating the surfaces with silica layers, reflecting that the SiO_2 layers can be act as protecting layers without destroying the optical properties of hematite particles. This means that the monodispersed and spherical SiO_2-coated Fe_2O_3 particles with high optical reflectivity at around ~750 nm will have important applications in display devices as band-pass red-color filter materials as well as functional inorganic pigments.

Conclusion

Nano-sized hematite, α-Fe_2O_3, particles are prepared by thermal decomposition of trinuclear acetato-hydroxo iron (III) nitrate complex, $[Fe_3(OCOCH_3)_7OH \cdot 2H_2O]NO_3$, at 400 °C. Subsequent coating with silica layers can be successfully achieved by a controlled hydrolysis and condensation reaction of TEOS on hematite surfaces with varying the TEOS concentration and pH. The homogeneous deposition of silica layers results in the formation of monodispersed and spherical composite particles with high optical properties, which are well suited for inorganic band-pass color filters and red pigments.

Acknowledgment. This work was supported by the KOSEF(Grant No. 2000-1-12200-002-3) and the Brain Korea 21 Project (1999).

References

1. Cornell, R. M.; Schwertmann, U. *The Iron Oxides*; VCH Publishers: New York, 1996; p 463.
2. Matijevic, E.; Scheiner, P. *J. Colloid Interface Sci.* **1978**, *63*, 509.
3. Sugimoto, T.; Sakata, K.; Muramatsu, A. *J. Colloid Interface Sci.* **1993**, *159*, 372.
4. Babes, L.; Denizo, B.; Tanguy, G.; Jeune, J. J.; Jallet, P. *J. Colloid Interface Sci.* **1999**, *212*, 474.
5. Matijevic, E. *J. Eur. Ceram. Soc.* **1998**, *18*, 1357.
6. Sugimoto, T.; Wang, Y.; Itoh, H.; Muramatsu, A. *Colloids and Surfaces A* **1998**, *134*, 265.
7. Ozaki, M.; Kratohvil, S.; Matijevic, E. *J. Colloid Interface Sci.* **1984**, *102*, 146.
8. Sugimoto, T.; Waki, S.; Itoh, H.; Muramatsu, A. *Colloids and Surfaces A* **1996**, *109*, 155.
9. Kominami, H.; Onoue, S.; Matsuo, K.; Kera, Y. *J. Am. Ceram. Soc.* **1999**, *82*, 1937.
10. Liu, X.; Ding, J.; Wang, J. *J. Mater. Res.* **1999**, *14*, 3355.
11. Ohno, K.; Kusunoki, T. *J. Electrochem. Soc.* **1996**, *143*, 1063.
12. Ohmori, M.; Matijevic, E. *J. Colloid Interface Sci.* **1992**, *150*, 594.
13. Chaneac, C.; Tronc, E.; Jolivet, J. J. *J. Mater. Chem.* **1996**, *6*, 1905.
14. Monte, F.; Morales, M. P.; Levy, D.; Fernandez, A.; Ocana, M.; Roig, A.; Molins, E.; O'Grady, K.; Serna, C. J.

Langmuir **1997**, *13*, 3627.
15. Ennas, G.; Musinu, A.; Piccaluga, G.; Zedda, D.; Gatteschi, D.; Sangregorio, C.; Stanger, J. L.; Concas, G.; Spano, G. *Chem. Mater.* **1998**, *10*, 495.
16. Liu, Q.; Xu, Z.; Finch, J. A.; Egerton, R. *Chem. Mater.* **1998**, *10*, 3936.
17. Wang, G.; Harrison, A. *J. Colloid Interface Sci.* **1999**, *217*, 203.
18. Stark, K. *J. Inorg. Nucl. Chem.* **1960**, *13*, 254.
19. Barr, T. L. *J. Phys. Chem.* **1978**, *82*, 1801.
20. Allen, G. C.; Curtis, M. T.; Hooper, A. J.; Tucker, P. M. *J. C. S. Dalton Trans.* **1974**, 1525.